Lawrence Berkeley Laboratory
UNIVERSITY OF CALIFORNIA

Accelerator & Fusion
Research Division

Invited Paper presented at the 12th International
Free Electron Laser Conference, Paris, France,
September 17–21, 1990, and to be published
in the Proceedings

Stability and Performance of CDRL-FEL

K.-J. Kim and M. Xie

November 1990

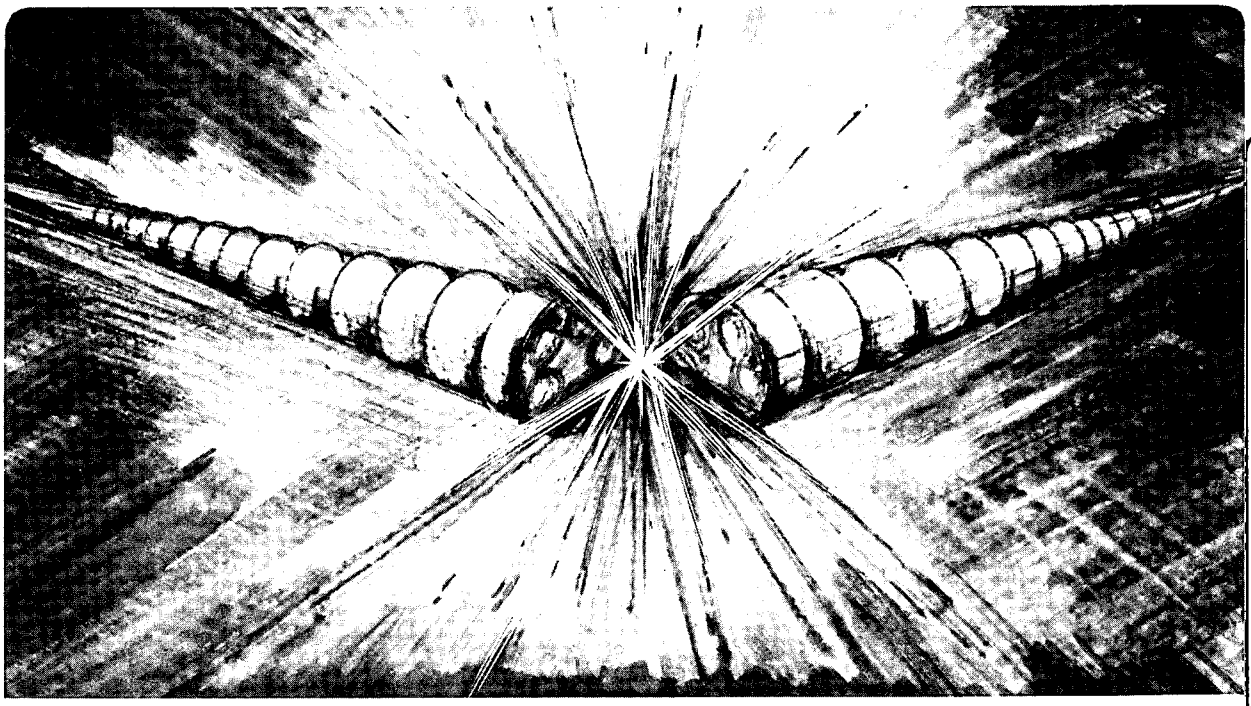

Prepared for the U.S. Department of Energy under Contract Number DE-AC03-76SF00098.

DISCLAIMER

LBL-29853
ESG-111

Stability and Performance of CDRL-FEL*

Kwang-Je Kim and Ming Xie

Lawrence Berkeley Laboratory
1 Cyclotron Road
Berkeley, California 94720

Invited Paper Presented at the 12th International Free Electron Laser Conference
Paris, France, September 17 - 21, 1990

*This work is supported by the Director, Office of Energy Research, Office of Basic Energy Sciences, Materials Sciences Division, of the U. S. Department of Energy under Contract No. DE-AC03-76SF00098.

Abstract:

We study the performance of a proposed infrared free electron laser at Lawrence Berkeley Laboratory, which would be a user facility and therefore has a unique set of requirements in intensity, spectrum and stability. The output performance in intensity and spectrum, and methods to optimize the performance, are studied in detail. The effect of the electron beam fluctuation on FEL stability is carefully evaluated to set a tolerance for the accelerator design. Use of intracavity gratings is studied as a means of further improving the spectral purity and stability.

1. Introduction

The Infrared Free Electron Laser (IRFEL) for the Chemical Dynamics Research Laboratory (CDRL), referred to as the CDRL-FEL, is being designed at Lawrence Berkeley Laboratory as a user facility serving a community of chemists. An overview of the accelerator-FEL system design is presented in a separate report[1]. The major parameters are listed in Table 1. Being a user facility, the CDRL-FEL must provide extremely stable, broadly tunable and narrow bandwidth radiation over the wavelength range of 3 to 50 μm. As a part of the design effort, we are undertaking a detailed study of the FEL characteristics, with the view of understanding how to optimize the electron beam parameters and optical cavity configurations to achieve the required performance and stability in spectral purity and output intensity. This paper is a report of the progress in this direction.

The study in this paper is based on theoretical analysis as well as numerical calculation. The numerical calculation was performed by using a simulation code originally developed by S. Benson[2]. The code is based on one dimensional FEL equations, the three dimensional effects being taken into account by means of suitable filling factors.

Table 1

Major Parameters of CDRL-FEL

Optical Beam:	
Wavelength range	$3\mu m < \lambda < 50\ \mu m$
Micropulse energy	$100\ \mu J$ at λ - $3\ \mu m$
Micropulse duration (τ, FWHM)	10 (25) ps
Micropulse rep. rate	36.6 (18.3) MHz
Marcopulse duration	$100\ \mu s$
Macropulse rep. rate	60 Hz
Average power	20 W
Bandwidth ($\Delta\lambda/\lambda$)	10^{-3} for λ - 3μ, τ - 10 ps
Electron Beam:	
Maximum energy	56 MeV
Energy spread (FWHM)	0.5% (at 56 MeV)
Micropulse peak current	100 Amps
Normalized rms emittance	20 mm-mrad
Undulator (SmCO - Steel Hybrid):	
Period length (λ_u)	5.0 cm
Number of periods (N)	40
Optical cavity:	
Radius of curvature (R)	4.3 m
Cavity length (L)	8.2 m

Section 2 presents a study of the intensity and spectrum. An important parameter in optimizing the FEL performance is the so-called cavity detuning, which is the amount by which the length of the cavity is shorter than that required by the synchronism condition. By combining the simulation results with theoretical analysis, we have determined the value of the cavity detuning for which the sidebands are suppressed while maintaining high FEL efficiency. We find also that proper detuning removes the shot noise fluctuation. The optimized spectrum has a relative bandwidth corresponding to a coherent optical pulse whose length is about the same as that the electron pulse, about 10^{-3} for λ(wavelength) -3 μm and τ (FWHM pulse length)- 10 ps. In certain cases of long wavelengths, high gain and large detuning lead to optical pulses which extend significantly beyond the front end of the electron pulse. The bandwidth in such cases corresponds to an optical pulse which is longer than the electron pulse. We have calculated the FEL gain, bandwidth, pulse energy, etc., for various operating conditions of CDRL-FEL. The performance predicted by calculation meets the CDRL user requirements.

Crucial to the operation of the CDRL-FEL is the stability of the FEL, which is the subject of Section 3. The goal is to control the fluctuation in the FEL spectrum and the intensity to a level less than 10^{-3} and 10^{-1}, respectively. With an usual optical cavity without frequency filtering elements, the stability of the FEL output is mainly determined by the stability of the electron beam. The effect of the electron beam fluctuation is different according to whether it is faster or slower than the response of the FEL cavity. Slow fluctuation leads directly to the fluctuation of the FEL output characteristics and needs to be controlled tightly. Fast fluctuation, on the other hand, is similar in effect to inhomogeneous broadening such as the electron energy spread. Thus the tolerances for the fast fluctuation is also similar to those for the inhomogeneous broadening. We have studied numerically the amplitude and frequency dependence of the fluctuation effect by introducing a sinusoidal modulation in electron beam parameters in the simulation code. The results are in reasonable agreement with our theoretical understanding.

Use of intracavity gratings offers an opportunity to improve spectral purity and stability of the FEL output beyond the level possible by electron beam control alone. This is studied in Section 4. A grating in Littrow configuration can be used to suppress the sideband growth, stabilize the wavelength fluctuation, and at the same time provide some output coupling. We provide a simple analytical model that explains the role of the grating in wavelength stabilization. The prediction of the model agrees with the numerical calculations in which the grating is represented as a frequency filter. Our analysis shows that, with a proper choice of the grating parameters, the wavelength fluctuation can be reduced to a level of 10^{-4} or smaller. The gratings suitable for the wavelength region of the CDRL-FEL have large groove spacings to avoid an excessive pulse stretching. We derive a closed expression for the grating efficiency and show that the tuning range of an individual grating can be about 30 %. Finally, we point out some three dimensional effects, the study of which is in a very preliminary stage.

2. FEL Performance

In this section, we discuss the intensity and spectrum of the CDRL-FEL and methods to optimize these characteristics. The electron beam parameters in the calculation are those given in Table 1, except that the micropulse length was allowed to vary between 5 and 25 ps and the peak current between 50 and 100 A. The undulator parameters for some of the runs were N (number of the undulator periods) = 46 and λ_u (period length) = 4.3 cm , rather than N = 40 and λ_u = 5 cm as in the final version of CDRL-FEL.

2.1 Cavity Detuning, Sidebands and Power

For an FEL based on an RF accelerator, the length of the optical cavity L and the micropulse separation T are related by the following synchronism condition:

$$T = 2L/c , \qquad (1)$$

where c is the speed of light. It turns out that the the length of the optical cavity should be slightly shorter by an amount δL, usually referred to as the cavity detuning, than that determined by Eq.(1). The cavity detuning turns out to be an important parameter that can be adjusted to control the FEL performance. For a small detuning, the approach to saturation is slow and the spectrum exhibits sidebands and sometimes even chaotic modes. The appearance of the sidebands and chaotic modes is a high intensity phenomenon and is related to the synchrotron oscillation in the ponderomotive potential [3], [4]. These undesirable effects can be avoided by adjusting the amount of the cavity detuning [5].

Figure 1 illustrates the effect of the cavity detuning on FEL spectrum. The spectrum contains strong side bands for a small detuning, δL - 18 μm, as shown in Fig. 1a, while it is well behaved with a single peak for a large detuning, δL - 89 μm, as shown in Fig. 1.b.

The fraction η of the electron beam's kinetic power P_{beam} converted into the optical power P_{opt} generated by the FEL interaction is called the efficiency. Thus

$$P_{opt} - \eta P_{beam} . \tag{3}$$

A simple argument shows that the efficiency is about $1/2N$, where N is the number of the undulator periods. However, the result of numerical simulation indicates that when the sideband development is suppressed for higher spectral purity, the maximum efficiency is about one half of that given by Eq.(3).

We have calculated the FEL efficiency as a function of the cavity detuning for various cases of CDRL-FEL. Such a curve is usually referred to as the detuning curve. Figure 2 is an example of the detuning curve for the case λ - 10 μm. From this figure, we can divide the value of the cavity detuning into three different regions:

Region(I) with a small value of δL, characterized by appearance of sidebands and chaotic modes, with high efficiency $\eta > 0.5/2N$,

Region(II) with a medium value of δL, characterized by a good spectrum with a reasonable efficiency η- (0.4 - 0.5)/2N, and

Region(III) with a large value of δL, characterized by a good spectrum but with a low efficiency η <0.4/2N. For the particular example of Fig. (2), regions (I), (II) and (III) correspond respectively to the detuning ranges of $\delta L < 40\ \mu m$, $40\ \mu m \leq \delta L \leq 100\ \mu m$, and $\delta L > 100\ \mu m$. Region (I) is not suitable for application requiring high spectral purity. On the other hand, the efficiency in region (III) is too low. Thus the optimal detuning is therefore in region (II). The distinct characteristics of different regions of the detuning curve were clearly demonstrated by LANL experiments [5].

The need for cavity detuning can also be explained by the FEL "lethargy" phenomenon [6]. Because of the slippage effect, i.e., the fact that the optical pulse moves past the electron pulse in traversing the FEL interaction region, the amplication is slightly stronger in the trailing part of the optical pulse. The centroid of the optical pulse will therefore fall behind the electron pulse steadily during the FEL evolution unless the effect is corrected by the detuning δL. The effect is analytically calculated within the supermode theory [7]. By examining the prediction of that theory [8], [9], we find that the value of the cavity detuning can be divided into the following three regions. The region $\delta L \leq 0.1 g\lambda N$ in which the gain of the fundamental supermode is small and the higher order modes can have a positive gain, the region $0.1 g\lambda N \leq \delta L \leq 0.2 g\lambda N$ in which the gain of the fundamental supermode is maximum and the higher order modes are suppressed, and the region $\delta L > 0.2 g\lambda N$ in which the gain of the fundamental supermode is small and the higher order modes are suppressed. Thus, it is apparent that there is a close connection between the growth of the sidebands with that of the higher order supermodes. If we connect these two phenomena, we can write down analytical expressions for the limits of different detuning regions discussed in the previous paragraph. In particular, the detuning range corresponding to region (II), where the FEL operation is optimum, is

$$0.1g\lambda N \leq \delta L \leq 0.2\, g\lambda N . \tag{4}$$

We have confirmed the validity of this identification by examining the detuning curves of several different cases of the CDRL-FEL, including the one in Fig.(2).

Denoting the total round trip loss by α, the intracavity power is given by

$$P = \frac{P_{\text{out}}}{\alpha} = \frac{\eta}{\alpha} P_{\text{beam}} . \tag{5}$$

The intracavity optical elements must be designed so that they can withstand the power level given by P.

The loss α consists of the useful loss α_c due to outcoupling and other loss α' :

$$\alpha = \alpha_c + \alpha' \tag{6}$$

Thus, the useful output power is given by

$$P_c = \left(\frac{\alpha_c}{\alpha}\right) \eta P_{\text{beam}} . \tag{7}$$

The ratio α_c/α depends on the details of the outcoupling. For the hole coupling scheme being studied for the CDRL-FEL [10], this ratio is about 0.5. Therefore the efficiency to the useful output in the region (II) will be about $1/8N$.

2.2 Fluctuation due to Shot Noise

As the FEL signal evolves from the initial spontaneous radiation, which is a phenomenon due to shot noise, the saturated FEL output is expected to exhibit some shot to shot fluctuation. Thus, for example, the position of the spectral peak can fluctuate within a fraction of the gain bandwidth. However, it is found from simulation calculation that the effect of the shot noise fluctuation on the saturated spectrum can be removed by cavity detuning.

We compare in Fig.(3) the spectra corresponding to different random seeds that characterize the shot noise in Benson's code. Figure (3.a) is a collection of four spectra corresponding to four different seeds when the detuning is small. The fluctuation of the spectrum due to the shot noise is evident in this case. On the other hand, the fluctuation for the case of a larger detuning is hardly visible as shown in Fig. (3.b), where the spectra corresponding to different seeds overlap and appear as a single spectrum.

2.3. Spectrum

The effect of FEL gain (per one round trip) on the shape of the optical spectrum can be modeled by a multiplicative factor[11]

$$G_0(\omega) = \mathrm{Exp}\left[-\frac{g}{2}\left(\frac{\omega-\omega_0}{\sigma_0}\right)^2\right] \quad . \tag{8}$$

Here ω_0 is the resonance frequency and σ_0 is the gain bandwidth, approximately given by

$$\sigma_0 \approx \omega_0/2N \quad . \tag{9}$$

The spectrum after nth round trip is determined by the function $(G_0(\omega))^n$. Thus, the evolution of FEL bandwidth in the optical cavity is given by

$$\frac{\Delta\lambda}{\lambda} \sim \frac{1}{N\sqrt{gn}} \tag{10}$$

where n is the number of round trips. Eventually the bandwidth becomes that corresponding to a coherent optical pulse extending the length τc of the electron beam micropulse:

$$\frac{\Delta\lambda}{\lambda} \sim \frac{\lambda}{c\tau} \quad . \tag{11}$$

Equation (11) is referred to as the electron beam transform limited (EBTL) bandwidth [12]. In order to achieve the EBTL bandwidth, it is necessary to prevent the growth of the sidebands by , for example, a proper cavity detuning as discussed before.

The approach to the EBTL bandwidth, Eq.(11), is slow. Figure 4.a shows the spectrum for the case λ -3 μm and τ - 10 psec at n - 150. Although the FEL intensity for this n is almost at its saturated value, the spectrum is still evolving and exhibits some structure. The spectrum reaches the steady state after n - 500 as shown in Fig. 4.b. We should therefore distinguish the intensity saturation and the spectrum saturation in the FEL evolution[11]. The length of the electron beam macropulses needs to be sufficiently long to allow the FEL to reach the spectrum saturation. The time for the spectrum saturation for the case of Fig.(4.b) is about 25 μs.

We have observed that the optical pulses can in some cases develop a long exponential tail in the front end. This happens when the gain is sufficiently high and the detuning is properly chosen and is caused by the spilling of the optical energy through the front end of the electron pulse. In Fig. (5), we show the temporal profiles of the optical pulses for two cases, one for λ - 3 μm and one for λ - 35 μm for the same electron pulse length τ - 10 ps, are compared. In the first case, the length of the optical pulse is essentially the same as that of the electron pulse, while in the second case it is several times longer. Figure 6 shows the corresponding spectral profiles. We see that the spectral bandwidth of the case λ - 35 μm is almost the same as that for λ - 3 μm. Note, however, that the spectral shape due to an exponential tail is Lorentzian, which has a long tail in the frequency domain and thus may be undesirable for certain applications.

2.4 Summary of Performance for IRFEL for CDRL

Tables 2 and 3 summarize the performance of the CDRL-FEL obtained from simulation calculation. The electron beam parameters in this calculation are those listed in Table 1. The undulator design is of the standard Halbach type based on the SmCO-steel hybrid [13]. With λ_u-5 cm, the FEL wavelength at a fixed electron energy can be scanned between λ-λ_{min} and λ-λ_{max}-2.15 λ_{min} by varying the magnet gap from 31.8 mm to 20.5 mm. Thus the entire wavelength range of 3 to 50 μm can be covered by running the accelerator at four different energies, E_e-55.3 MeV, 39.1 MeV, 27.7 MeV, and 19.6 MeV.

The net gain in the Tables is the total gain g minus the loss α(10 % in this case) at the beginning of the FEL evolution. It is seen that the gain has a sufficient margin for a reliable FEL operation, and also for possible additional losses, for example those associated with intracavity elements such as gratings. The magnitude of the relative electron energy spread in the calculation is 0.5 % at 55.3 MeV, and is inversely proportional to the electron energy. It is found that the gain reduction is significant at lower electron energies, but the effect is more than balanced by other effects that increase the gain at longer wavelengths.

The output characteristics in Tables 2 and 3 are the optimized performance with respect to the cavity detuning. The optimization is achieved by comparing the output at several value of the cavity detuning near δL-0.1 gλN, i.e., the lower end of the region (II) given inEq.(4), and choosing the one with maximum output energy(or efficiency) without the sideband development. The value of δL corresponding to the optimum performance is listed in the Tables and agrees approximately with the formula δL - 0.1 gλN, except in the long wavelength cases. The discrepancy for the long wavelengths is due to the pulse length correction factor[9] and presumably also due to high gain effect which is beyond the supermode theory.

The spectral bandwidth in the Tables is consistent with the electron beam transform limited value, Eq. (12), for short wavelengths around 3 μm, about 10^{-3} for τ-10 ps and 5×10^{-4} for τ-25ps. For longer wavelengths near 50 μm, we see clearly the evidence of the

front tail due to the spilling phenomena.

The last column in the Table 2 and 3 gives the useful output energy in a single optical micropulse.

Table 2.

Performance of CDRL-FEL

For electron pulse length - 10 ps, pulse charge - 1 nC,

Total loss - 10%, outcoupling - 5%

λ (μm)	E_e (MeV)	Net Gain (%)	δL (μm)	$\Delta\lambda/\lambda$ (%)	Pulse Energy (μJ)
3	55.3	43	9	0.11	147
6.45	55.3	146	30	0.16	156
6	39.1	75	20	0.19	113
12.9	39.1	194	90	0.18	104
12	27.7	95	40	0.39	80
25.8	27.7	266	150	0.17	75
25	19.6	125	80	0.41	49
53.75	19.6	250	250	0.20	50

Table 3

Performance of CDRL-FEL

For electron pulse length - 25 ps, pulse charge - 2.5 nC,

Total loss - 10%, outcoupling - 5%

λ (μm)	E_e (MeV)	Net Gain (%)	δL (μm)	$\Delta\lambda/\lambda$ (%)	Pulse Energy (μJ)
3	55.3	42	9	0.05	346
6.45	55.3	145	40	0.09	373
6	39.1	81	20	0.08	282
12.9	39.1	246	80	0.18	241
12	27.7	111	40	0.16	194
25.8	27.7	310	180	0.38	163
25	19.6	144	100	0.41	112
53.75	19.6	318	300	0.23	118

3. FEL Stability

In order to fully exploit the spectral purity of FEL, the fluctuation in the spectrum should be smaller than the bandwidth. The stability of the output intensity is also important for many experiments. In designing the CDRL-FEL, we put special emphasis in the stability of the FEL output. In this section we study the fluctuation in the radiation characteristics caused by the fluctuation in electron beam parameters for FEL operation without intracavity gratings. The case with gratings is the subject of Section 4.

3.1 Requirement on Electron Beam Stability

The effect of electron beam fluctuation on FEL performance is different according to whether the fluctuation occurs with a time scale faster or slower than the response time of FEL. The FEL response time is given by the cavity Q time, t_Q-2L/cα. In the frequency domain, the characteristic frequency f_Q is related to t_Q by $2\pi f_Q t_Q - 1$. For the case of CDRL-FEL, for which L-8.2 m and α is typically about 0.1, we have t_Q - 0.5 μsec or f_Q-0.3 MHz.

Thus we will distinguish between the slow fluctuation and the fast fluctuation as follows: The slow fluctuation is the change in the electron beam parameters occurring in a time scale longer than 0.5 μsec, or with frequencies smaller than 0.3 MHz. The effect of the slow fluctuation on FEL output is equivalent to a DC change in the electron beam parameters. The fast fluctuation is the change in the electron beam parameters occurring in a time scale shorter than 0.5 μsec or with frequencies higher than 0.3 MHz. The main effect of fast fluctuation is in the reduction of the gain, similar to energy spread and emittance.

The requirements on slow fluctuations are as follows: Since we require the wavelength fluctuation $\delta\lambda/\lambda$ to be less than 10^{-3}, and since the wavelength fluctuation is twice that of the electron energy fluctuation, the requirement on the slow fluctuation in the electron energy is

$$\delta E/E < 5x10^{-4}. \tag{12}$$

The fluctuation in the timing between the electron micropulse δT is equivalent to the fluctuation in the cavity length or detuning via the relation $\delta T = 2\delta L/c$. In view of the discussion in Subsection 2.1, the fluctuation in δL should lie in the region(II) of the detuning curve , the width of which is $0.1\, g\, \lambda N$ (See Eq.(4)). The most stringent requirement comes from the short wavelength case, $\lambda = 3\ \mu m$. Taking $g = 1$, we find that the allowed range of the slow fluctuation δT is

$$\delta T - 2\delta L/c < 0.1 \text{ ps} . \tag{13}$$

Notice that this is a requirement on the *difference* of the micropulse arrival times. It is thus equivalent to the requirement on the error of the RF frequency δf_{RF}:

$$\frac{\delta f_{RF}}{f_{RF}} < 2 \times 10^{-6} . \tag{14}$$

The fluctuation δQ in the pulse charge Q has a direct influence on the micropulse intensity. It also has an indirect influence on the FEL wavelength fluctuation through a change of the electron beam energy via beam loading effect. The requirement through the latter effect turns out to be more stringent, and leads to

$$\delta Q/Q < 0.02. \tag{15}$$

The tolerance on fast fluctuation, with frequencies higher than 0.3 MHz, in the electron beam energy is given by the the energy spread. The tolerance on the fast fluctuation of the micropulse timing δT is determined by requiring that the overlapping of the optical beam with

the electron beam be accurate within one tenth of the pulse length. The tolerance on the fast fluctuation is therefore

$$\frac{\delta E}{E} \leq 5 \times 10^{-3} \ , \delta T \leq 1 \text{ ps} . \tag{16}$$

This is an order of magnitude less stringent than the tolerance on the slow fluctuation.

In addition, the electron beam must be transversely stable for the stability of the output. The user requirement on the fluctuation in the position δx and the angle $\delta x'$ is

$$\delta x \leq 0.1 \, \sigma_x \qquad \delta x' \leq 0.1 \, \sigma_{x'} \ , \tag{17}$$

where σ_x and $\sigma_{x'}$ are, respectively, the rms value of the transverse size and angular divergence.

The required electron beam stability described above is very demanding but can be achieved with current technology by employing passive regulation as well as active feedback and feedforward control[1].

Stabilizing the wavelength beyond the 10^{-3} level requires methods other than the electron beam control, such as using intracavity gratings. This will be discussed in section 4.

3.2 Simulation Calculation of FEL Response to Fast and Slow Fluctuations

We have calculated the fluctuation in the FEL output caused by the fluctuation in the electron beam parameters. Since the effect is sensitive to the fluctuation frequency, we consider a single Fourier component at a time. Thus we consider the following sinusoidal modulation in the electron beam energy δE and the spacing between the micropulses δT:

$$\delta T = \frac{1}{2} (\delta T)_{p\text{-}p} \cos 2\pi f t \ , \tag{18a}$$

$$\frac{\delta E}{E} = \frac{1}{2}\left(\frac{\delta E}{E}\right)_{p\text{-}p} \cos 2\pi f t \ . \qquad (18b)$$

Here, the subscript p-p refers to the peak to peak amplitude.

Figure 7 shows the variation of the FEL intensity, for several values of the modulation frequency f, as a function of the round trip pass number when δT is modulated according to Eq.(18a). The amplitude of the intensity variation as a function of f is shown in Fig. 8. It appears that the amplitude is inversely proportional to f, a physically reasonable result. According to Fig. 8, a sinusoidal timing modulation with peak to peak amplitude of 0.1 psec gives rise to an intensity modulation larger than 10% if the modulation frequency is smaller than 0.3 MHz. This is in agreement with the general discussion in previous Subsection.

Figure 9 shows amplitude of the intensity modulation as a function of f, when the electron beam energy is modulated according to Eq.(18b) with a peak to peak modulation amplitude of 0.05%. According to this figure, the frequency component between f - 0.1 MHz and f - 0.25 MHz should be suppressed in order to limit the intensity modulation to be less than 10%. This is again consistent with the previous discussion.

We show in Fig. 10 the wavelength modulation caused by the same modulation in energy as in Fig.9. It is seen that only very slow fluctuation, with frequencies smaller than 0.05 MHz, contributes to wavelength fluctuation larger than 0.1 %. It turns out that the effect of the timing fluctuation on FEL wavelength is not significant.

To be complete, it is necessary to study the total effect of the electron beam fluctuations characterized by the respective spectral densities. Such an analysis is beyond the scope of he present simulation calculations. However, it is reasonable to expect that the result will lead to the requirements on the slow and the faster fluctuations as discussed in Subsection (3.1).

4. Intracavity Gratings for Further Reduction of Wavelength Fluctuation

Intracavity dispersive elements such as gratings can be useful for sideband suppression and for wavelength stabilization beyond the level possible by the electron beam control alone. A schematic of the optical cavity with a grating in Littrow configuration is illustrated in Fig. (11). Here, the light reflected in the first order remains in the cavity while the reflection in the 0th or 2nd order provides a convenient outcoupling mechanism. A proof-of-principle experiment using gratings in FEL for sideband suppression[14] and for wavelength stabilization[15]was carried out at LANL.

The reason why an intracavity grating can reduce the wavelength fluctuation may be understood as follows: In analogy with Eq.(8), we represent the effect of a grating on the spectrum by the following filter function, ignoring three-dimensional effects:

$$G_g(\omega) = \mathrm{Exp}\left[-\frac{1}{2}\left(\frac{\omega-\omega_g}{\sigma_g}\right)^2\right] \tag{19}$$

where σ_g is the grating bandwidth and ω_g is the frequency for which the first order efficiency is maximum. The combined effect of the FEL gain and the grating on the spectrum is then represented by the product $G_0(\omega)$ given by Eq. (8) and $G_g(\omega)$, and can be written as

$$G_0(\omega)G_g(\omega) = \mathrm{Exp}\left[-\frac{1}{2}\left(\frac{(\omega-\bar{\omega})^2}{\bar{\sigma}^2}\right)\right]\mathrm{Exp}\left[-\frac{1}{2}\left(\frac{(\omega_0-\omega_g)^2}{\sigma_0^2+\sigma_g^2}\right)\right], \tag{20}$$

where

$$\bar{\omega} = \frac{g\omega_0\sigma_g^2 + \omega_g\sigma_0^2}{\sigma_0^2 + g\sigma_g^2}, \tag{21}$$

$$\bar{\sigma} = \frac{\sigma_0 \sigma_g}{\sqrt{\sigma_0^2 + g\sigma_g^2}} \quad , \tag{22}$$

From the first exponential factor of Eq.(20), we see that the spectrum is centered around a new resonance frequency $\bar{\omega}$ given by Eq. (21), which is a weighted average of ω_0 and ω_g. Noting that ω_g is set by the grating equation and thus not affected by the electron energy fluctuation, one can derive from Eq. (21) that the wavelength fluctuation in the presence of the intracavity grating is related to the fluctuation in the absence of a grating, $\delta\omega_0/\omega_0$, by

$$\frac{\delta\lambda}{\lambda} = \frac{\delta\bar{\omega}}{\bar{\omega}} = \frac{g(\sigma_g/\sigma_0)^2}{1 + g(\sigma_g/\sigma_0)^2} \frac{\delta\omega_0}{\omega_0} \quad . \tag{23}$$

At saturation, the gain g in the above can be replaced by the loss α, which is typically 0.1 for CDRL-FEL. Thus, the wavelength fluctuation can be reduced by a factor 10 or more when $\sigma_g \leq \sigma_0$.

We have calculated the wavelength fluctuation caused by the electron beam modulation in the presence of the intracavity grating by introducing the frequency filter, Eq. (19), in Benson's code. The result is summarized in Fig. (12), which agrees qualitatively with the behavior predicted by Eq. (23). It is seen from the figure that the wavelength fluctuation can be reduced to 10^{-4} by choosing the grating bandwidth σ_g/ω_0 to be 1% or less.

Gratings with narrower bandwidths, or with finer grooves, will be better from the stability point of view. However, an excessive pulse stretching caused by a finer grating could lead to an unacceptable reduction in the FEL gain[14]. For a Littrow grating configuration, the rms pulse stretching per grating reflection is calculated to be

$$\sigma_{\Delta z} \sim \lambda\sigma_x/d \quad , \tag{24}$$

where σ_x is the rms beam size at the grating and d is the groove spacing. To avoid a significant gain reduction, $\sigma_{\Delta z}$ should be small compared to the electron pulse length. For CDRL-FEL, the requirement leads to a coarse grating with d ~ 0.1 mm for $\lambda \leq 10$ μm and even coarser for a longer λ.

For a coarse grating with a shallow groove depth, the grating efficiency can be calculated in a closed form by using an asymptotic form of the Rayleigh's expansion [16]. The result for the first order efficiency $|E_1|^2$ near the blaze frequency ω_g is as follows:

$$|E_1|^2 = (\sin \varepsilon/\varepsilon)^2 \; ; \; \varepsilon = \pi(\omega - \omega_g)/\omega_g \quad . \tag{25}$$

If we require the efficiency to be larger than 90%, a single grating can cover the wavelength range

$$-0.17 \leq \frac{\omega - \omega_g}{\omega_g} \leq 0.17 \quad . \tag{26}$$

Thus the total tuning range is about 34%.

The efficiency into the 0th or the 2nd order reflection is given by

$$|E_0|^2 = |E_2|^2 = \left(\frac{\varepsilon}{\pi}\right)^2 = \left(\frac{\omega - \omega_g}{\omega_g}\right)^2 \quad . \tag{27}$$

Therefore, up to about 3% of the FEL intensity can be coupled out in each order for external use at the edge of the tuning range, Eq. (26). However, according to Eq.(27), the efficiency vanishes quadratically as ω approaches ω_g.

Three dimensional effects could be important for FEL operation with intracavity gratings. For example, for a fixed grating, the optical axis corresponding to a wavelength $\lambda \neq \lambda_g$ (λ_g - wavelength corresponding to ω_g) is rotated by an angle θ with respect to the original axis, where θ is given by the following expression [17]:

$$\theta = \frac{L}{4(2R-L)}\left(\frac{\lambda - \lambda_g}{d}\right) \quad , \tag{28}$$

where R is the radius of the curvature of the grating. The rotation of the optical axis can excite a walking mode around the new axis [18],[19], and should be limited to be smaller than, for example, the mode divergence angle. The analysis of these effects is in progress.

5. Acknowledgments

We thank Steve Benson for generously providing us with his code and for many critical remarks, Dodge Warren and John Goldstein for illuminating discussions on experimental and theoretical understanding of FEL stability, and Swapan Chattopadhyay for helpful suggestions and critically reading the manuscript .

References

[1] K.-J. Kim, et. al., " Design Overview of a Highly Stable IRFEL at LBL ", these proceedings.

[2] S. V. Benson," Diffractive Effects and Noise in Short Pulse Free-Electron Lasers", Ph.D dissertation, Department of Physics, Stanford University (1985).

[3] N.M. Kroll and M.N. Rosenbluth, Physics of Quantum Electronics, Vol 7(Addison-Wesley, Reading, MA,1980)147.

[4] J. C. Goldstein, Proc. SPIE 453 (1984)2.

[5] R.W. Warren, J.C. Goldstein and B.E. Newnam, Nucl. Instr. Meth., A 250(1986)19; R.W. Warren, J.C. Goldstein, Nucl. Instr. Meth., A 272 (1988) 155

[6] See for example, F.A. Hopf, T.G. Kuper, G.T. Mooreand M.O. Scully, Physics of Quantum Electronics, Vol 7 (Addison-Wesly, Reading, MA, 1980) 31

[7] G. Dattoli, A. Marino and A. Renieri, Opt. Commun. 35 (1980) 407 ; P. Elleaume,

IEEE J. Quantum Electron. QE-12 (1985) 1012

[8] G. Dattoli, A. Marino, A. Renieri and F. Romanelli, IEEE J. Quantum Electron. QE-17 (1981) 351; G. Dattoli, et. al., Nucl. Instr. Meth., A 285 (1989) 108

[9] We are assuming here that the slippage distance $N\lambda$ is small compared to the electron bunch length σ_z. If this is not true, the expression for δL should be corrected by the factor $1/(1+N\lambda/3\sigma_z)$. See Ref.[8].

[10] M. Xie and K.-J. Kim, " Hole Coupling Resonators for FELs", these proceedings.

[11] K.-J. Kim, " The Evolution and Limits of Spectral Bandwidth in FELs ", these proceedings.

[12] The condition for obtaining the EBTL bandwidth is that the FEL saturation takes place at strong field where the intensity dependent gain reduction bedcomes significant. See Ref [11]

[13] K. Halbach, J. Phys. (Paris) 44, (1983) C1-211.

[14] J.E. Sollid, et. al., Nucl. Instr. Meth., A 285 (1989) 147 ; J. E. Sollid, D.W. Feldman and R.W. Warren, Nucl. Instr. Meth., A 285 (1989) 153

[15] D.W. Feldman, Private communications.

[16] E.G. Loewen, M. Neviere and D. Maystre, J. Opt. Soc. America, Vol 68 (1978) 496

[17] We thank R.W. Warren for his help in deriving Eq.(28)

[18] W.M. Grossman and D.C. Quimby, Proc. SPIE, Vol 453 (1984) 86.

[19] R.W. Warren and B.D. McVey, Nucl. Instr. Meth., A 259 (1987) 154

Figure Captions

Figure 1. The FEL spectrum for different cavity detunings as a function of the relative frequency for $\lambda = 10$ μm, $\tau = 10$ ps and pulse charge = 1nC; [A] $\delta L = 18$ μm, [B] $\delta L = 89$ μm.

Figure 2. Extraction efficiency η as a function of cavity detuning. Three different regions are marked by (I),(II) and (III). The FEL spectrum at the detunings marked with [A] and [B] are shown respectively in Fig.1.A and Fig.1.B.

Figure 3. The FEL spectrum at saturation for four different shot-noise seeds. [A] $\delta L = 18$ μm, corresponding to the point marked with [A] in Fig.2. [B] $\delta L = 89$ micron, corresponding to the point marked with [B] in Fig.2.

Figure 4. The FEL spectrum for $\lambda = 3$ μm, $\tau = 10$ ps and pulse charge = 1nC at 150 passes in [A] and 500 passes in [B].

Figure 5. The temporal profiles of optical pulses $\tau = 10$ ps and pulse charge = 1nC at [A] $\lambda = 3$ μm and [B] $\lambda = 35$ μm.

Figure 6. The FEL spectrum corresponding to Fig.5; [A] $\lambda = 3$ μm and [B] $\lambda = 35$ μm.

Figure 7. The FEL intensity modulation caused by modulation in the bunch spacings.

Figure 8. The peak to peak amplitude of FEL intensity modulation as a function of frequency of modulation in bunch spacing.

Figure 9. The peak to peak amplitude of FEL intensity modulation as a function of frequency of modulation in electron beam energy.

Figure 10. The peak to peak amplitude of FEL wavelength modulation as a function of frequency of modulation in electron beam energy.

Figure 11. Schematic of the optical cavity with a grating in Littrow configuration.

Figure 12. The peak to peak amplitude of FEL wavelength modulation as a function of the intracavity grating bandwidth.

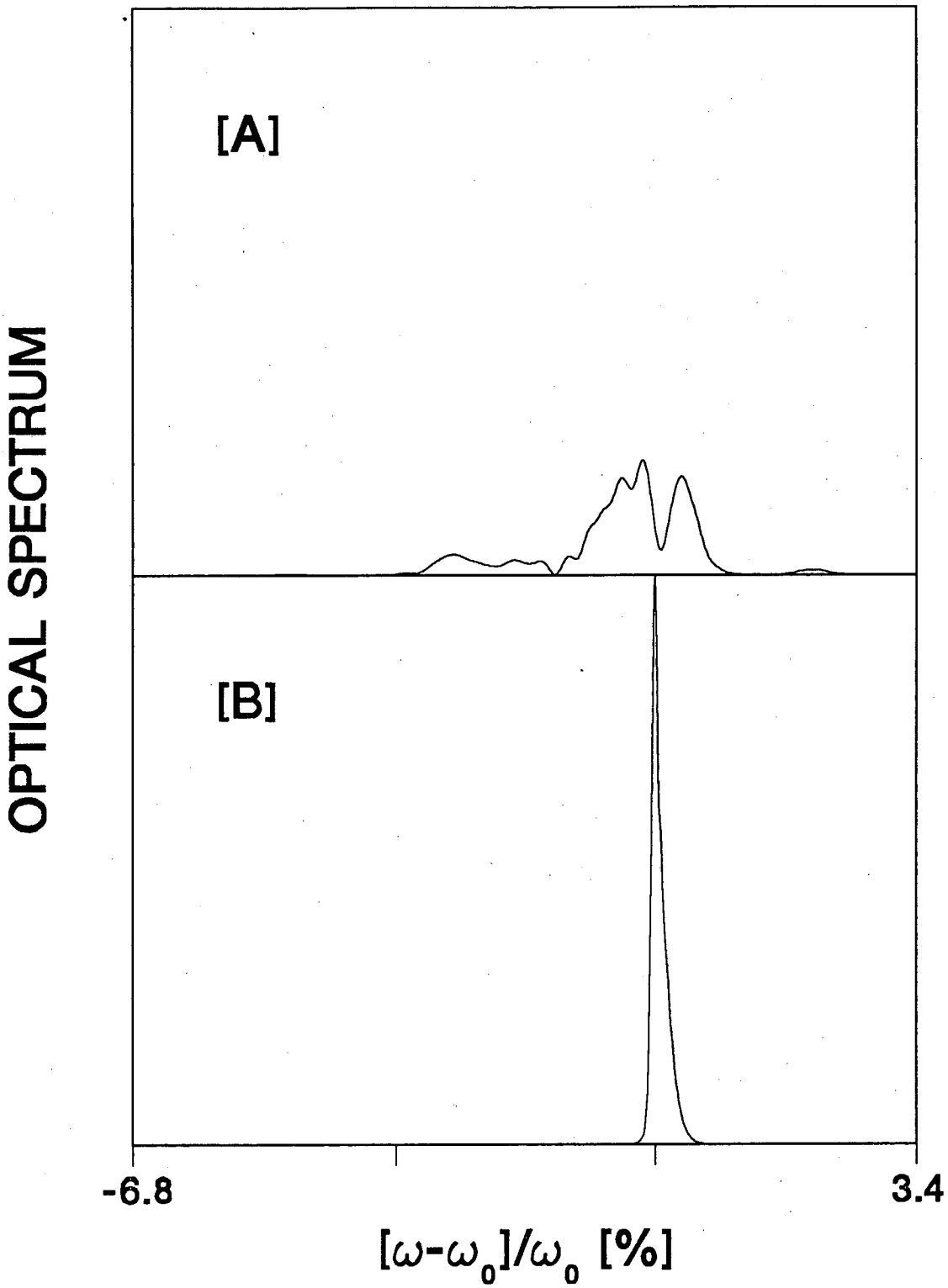

Fig. 1

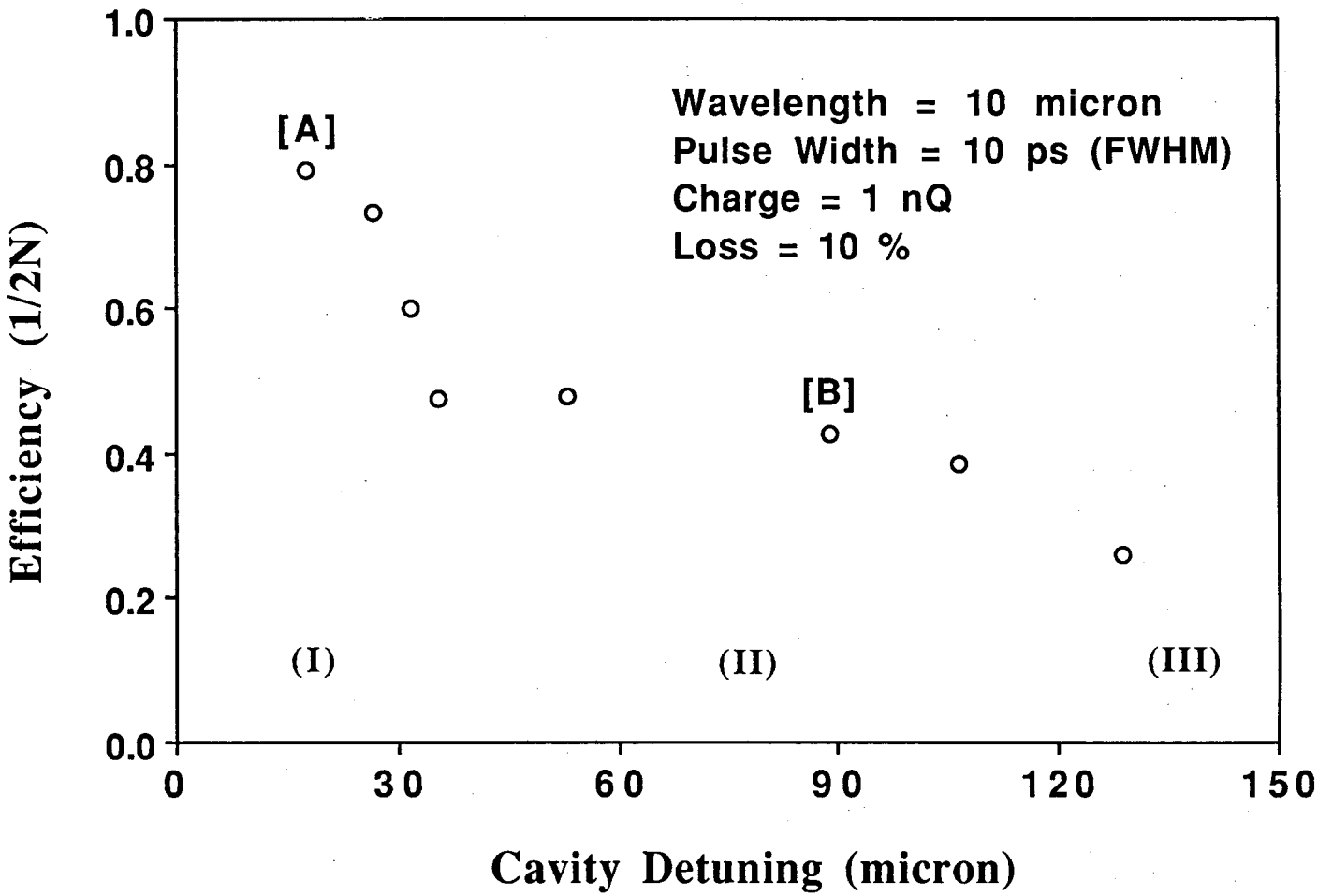
1.0
0.8
0.6
0.4
0.2
0.0
Efficiency (1/2N)
[A]
[B]
Wavelength = 10 micron
Pulse Width = 10 ps (FWHM)
Charge = 1 nQ
Loss = 10 %
(I)
(II)
(III)
0
30
60
90
120
150
Cavity Detuning (micron)

Fig. 2

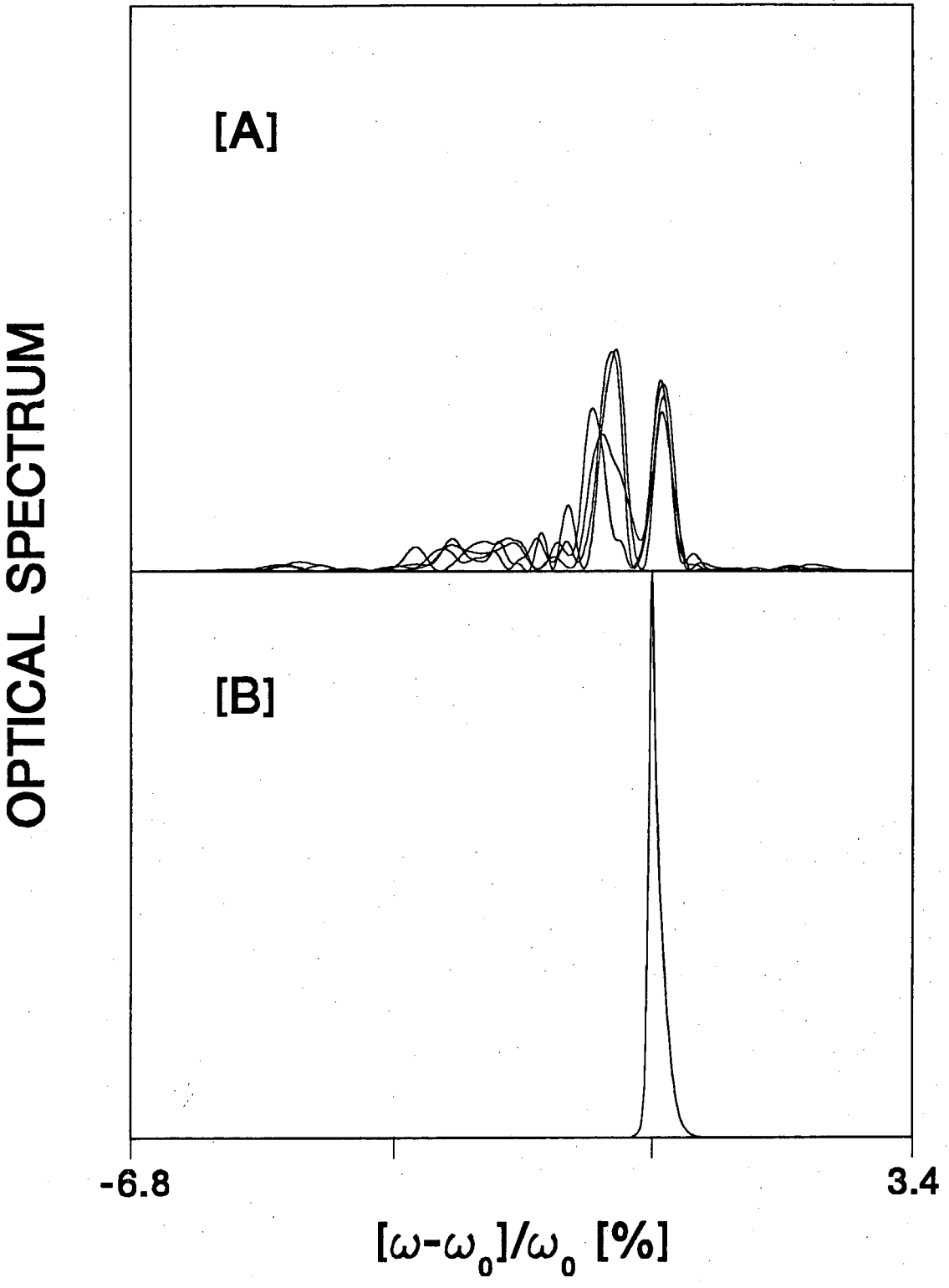

Fig. 3

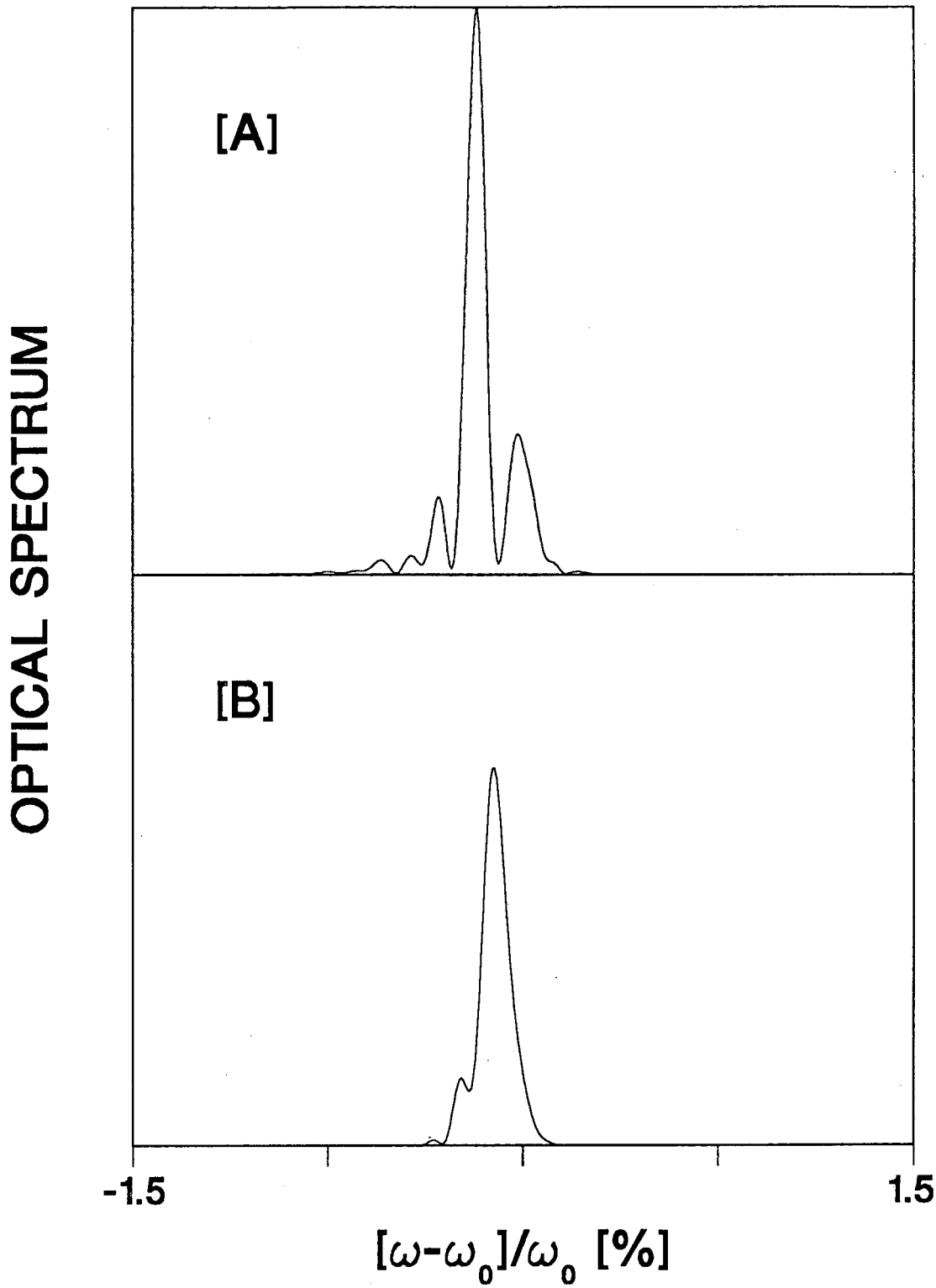

Fig. 4

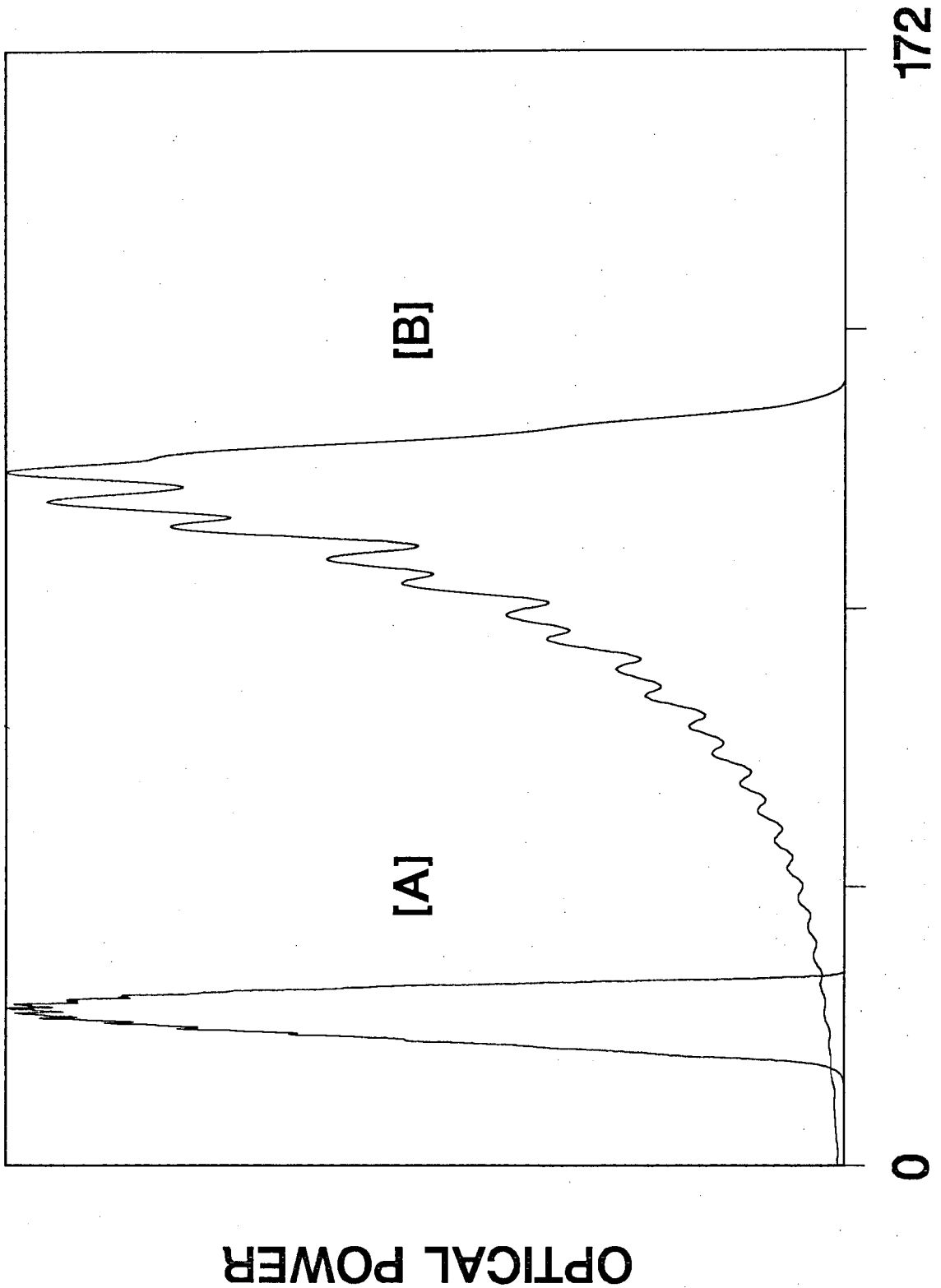

Fig. 5

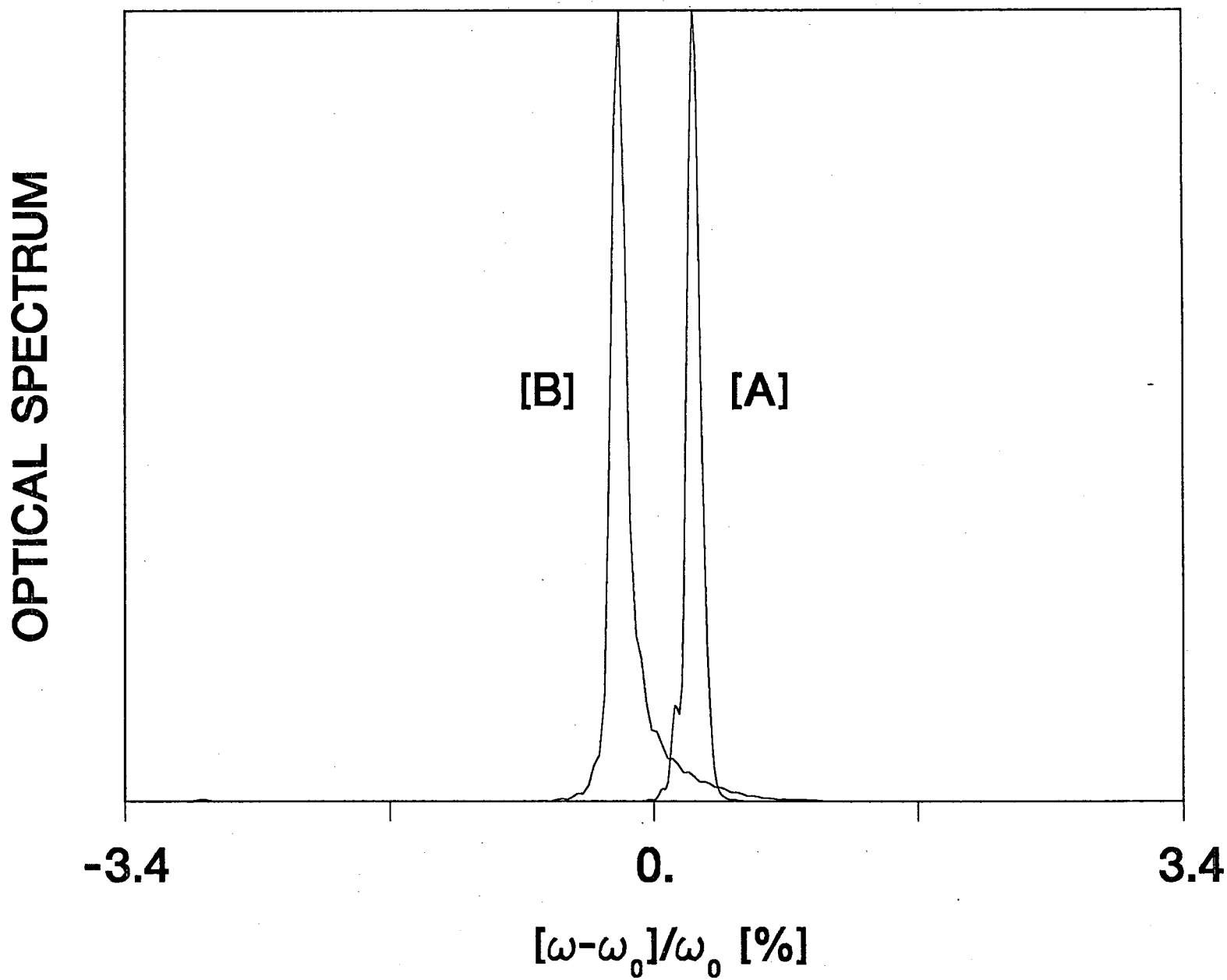

Fig. 6

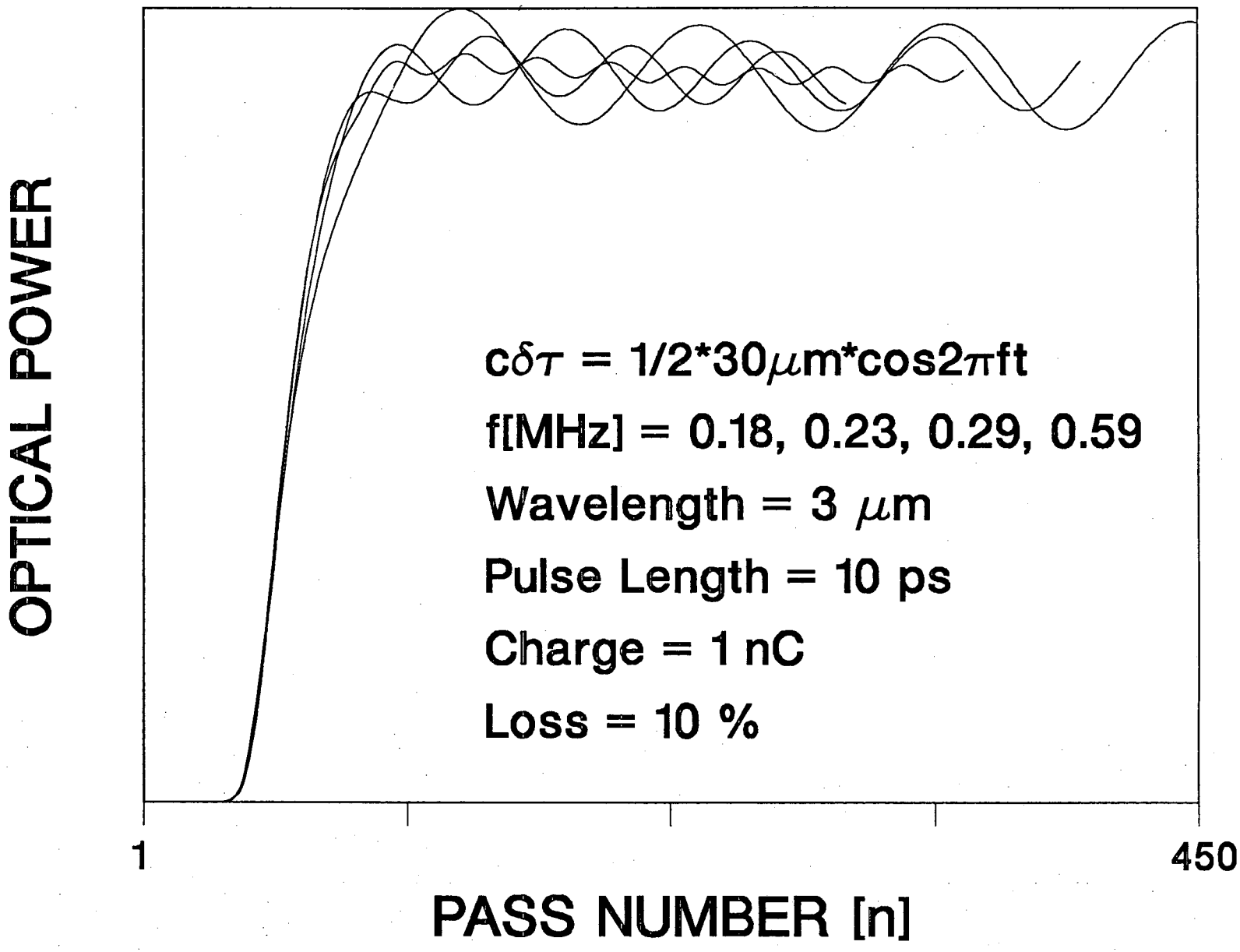
OPTICAL POWER
cδτ = 1/2*30μm*cos2πft
f[MHz] = 0.18, 0.23, 0.29, 0.59
Wavelength = 3 μm
Pulse Length = 10 ps
Charge = 1 nC
Loss = 10 %
1
450
PASS NUMBER [n]

Fig. 7

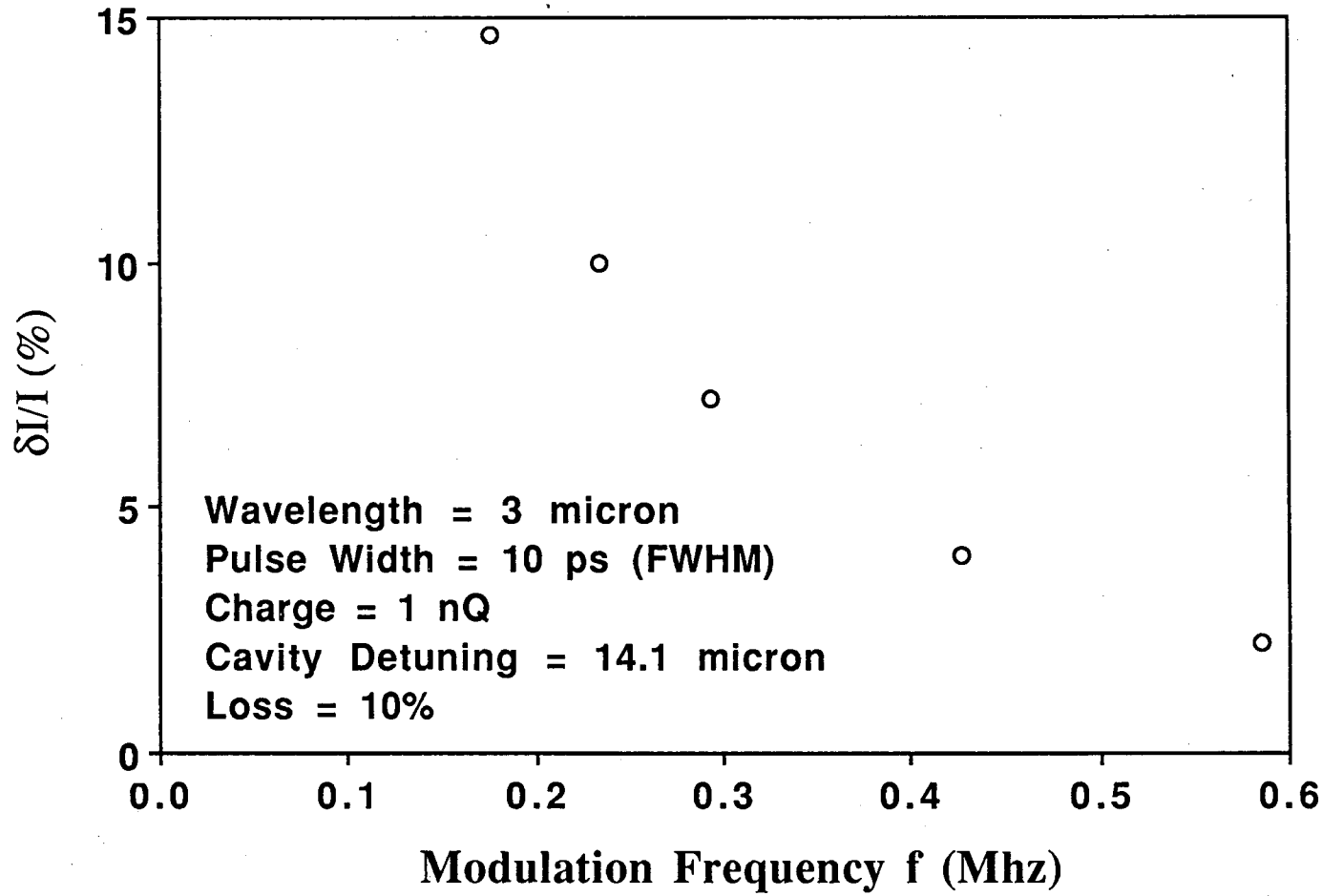
15
10
5
0
δI/I (%)
Wavelength = 3 micron
Pulse Width = 10 ps (FWHM)
Charge = 1 nQ
Cavity Detuning = 14.1 micron
Loss = 10%
0.0
0.1
0.2
0.3
0.4
0.5
0.6
Modulation Frequency f (Mhz)

Fig. 8

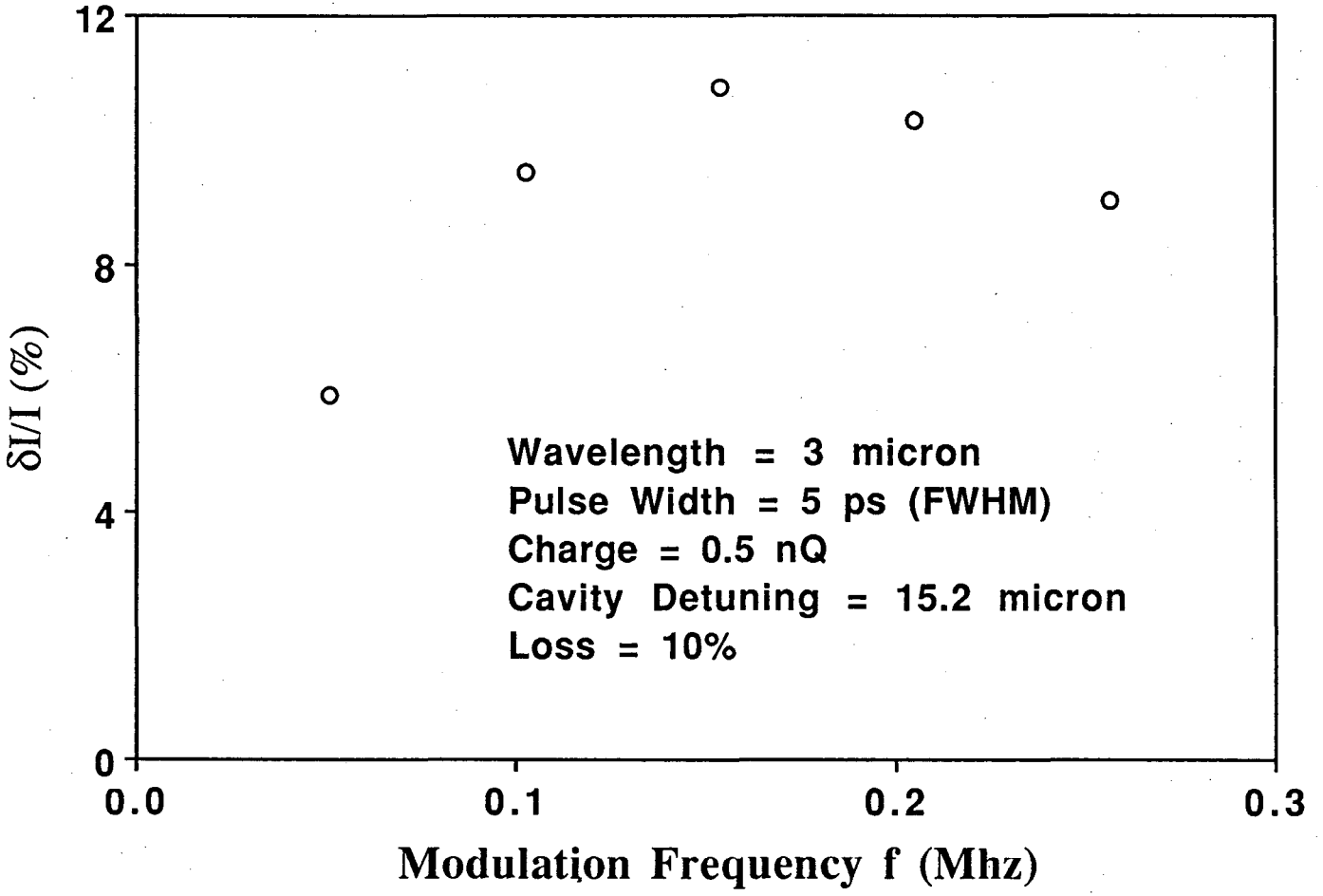
12
8
4
0
(%) ΔI/I
0.0
0.1
0.2
0.3
Modulation Frequency f (Mhz)
Wavelength = 3 micron
Pulse Width = 5 ps (FWHM)
Charge = 0.5 nQ
Cavity Detuning = 15.2 micron
Loss = 10%

Fig. 9

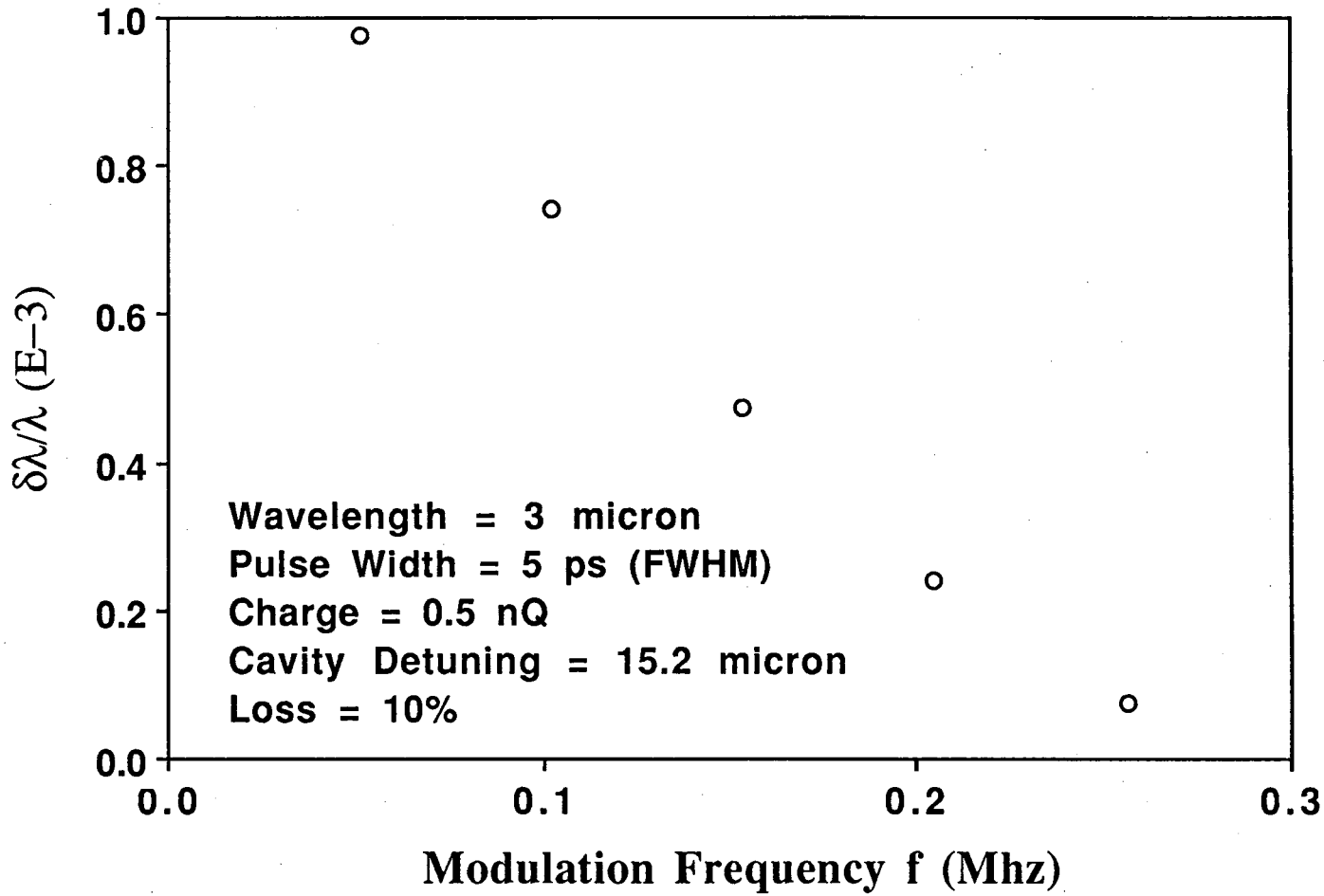
1.0
0.8
0.6
0.4
0.2
0.0
δλ/λ (E-3)
Wavelength = 3 micron
Pulse Width = 5 ps (FWHM)
Charge = 0.5 nQ
Cavity Detuning = 15.2 micron
Loss = 10%
0.0
0.1
0.2
0.3
Modulation Frequency f (Mhz)

Fig. 10

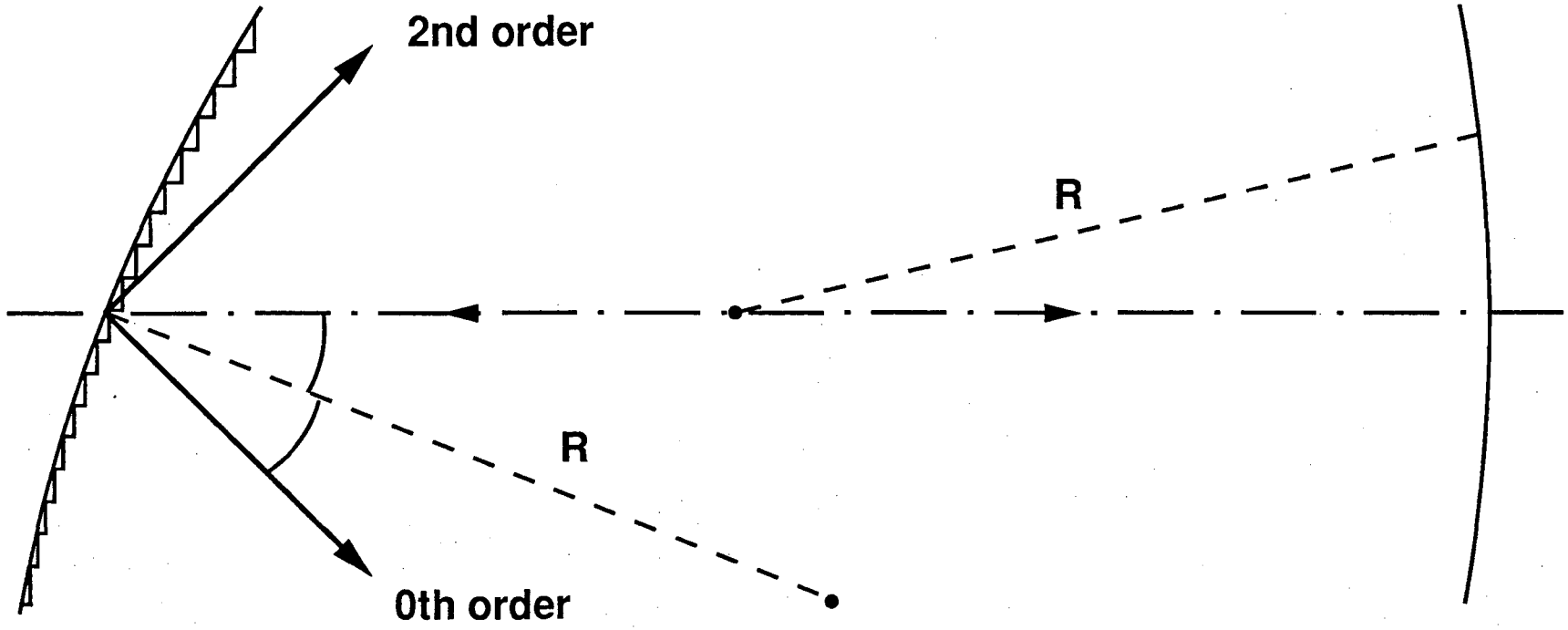

Fig. 11

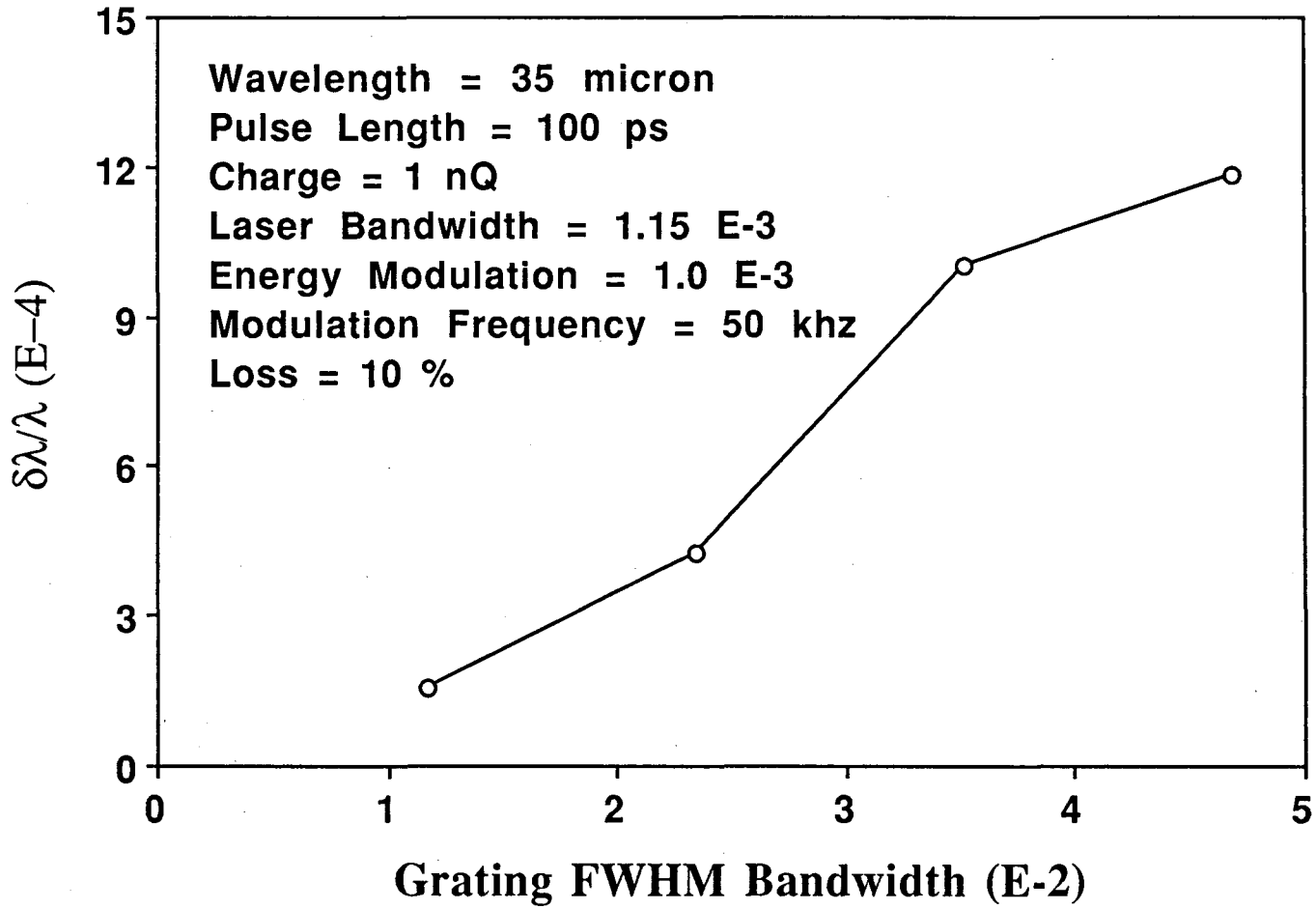
Wavelength = 35 micron
Pulse Length = 100 ps
Charge = 1 nQ
Laser Bandwidth = 1.15 E-3
Energy Modulation = 1.0 E-3
Modulation Frequency = 50 khz
Loss = 10 %
δλ/λ (E–4)
15
12
9
6
3
0
0
1
2
3
4
5
Grating FWHM Bandwidth (E-2)

Fig. 12

LAWRENCE BERKELEY LABORATORY
UNIVERSITY OF CALIFORNIA
INFORMATION RESOURCES DEPARTMENT
BERKELEY, CALIFORNIA 94720